48

Vacuum Arc Plasma Centrifuge for Element and Isotope Separation

M. GEVA, C. COHEN, O. DANZIGER, F. DOTHAN, L. FRIEDLAND, L. A. LEVIN, S. MAHARSHAK, AND J. L. HIRSHFIELD

Abstract—Vacuum arcs have been studied extensively in the past several decades with applications primarily in the areas of switching, vacuum remelting, and vapor deposition. Application of the vacuum arc for element and isotope separation has been studied recently and is reviewed in this paper. An arc was produced in a 30-cm-diameter 4-m-long cylindrical chamber with coaxially mounted electromagnets providing a 2.6-m-long constant axial magnetic field of up to 6 kG. The vacuum discharge between a solid cathode and a mesh anode was triggered electrically. A pulse-forming network (PFN) of 70-mΩ impedance provided nearly constant-current discharge pulses of several kiloamps and 6–12-ms duration. The magnetized plasma column, flowing axially from the anode with a typical velocity of 10^6 cm/s, rotated nearly as a solid body. This rotation was due to the $E \times B$ drift, produced by the axial magnetic field and the radial electric field across the column. A typical rotation frequency was 10^5 rad/s. The centrifugal effect due to the rotation caused a radial redistribution of ions within the plasma column, thereby producing elemental and isotope enrichment. The separation was observed to increase exponentially with the square of the radius. Enrichments of up to 300 percent were measured in a Cu–Zn plasma. The radial plasma density profile was found to be roughly Gaussian, with central electron densities of about 10^{13} cm^{-3}. The radial potential profile across the column was measured and found to be parabolic with radius. These observations can be accounted for by a steady-state multispecies fluid model of the rotating plasma.

I. Introduction

CENTRIFUGAL isotope separation in rotating plasma has been studied for more than four decades. Early work by Slepian [1] was followed by theoretical and experimental studies of Bonnevier [2], Lehnert [3], and many others. In its simplest form, the plasma centrifuge consists of a plasma column in a cylindrical vessel with an externally imposed axial magnetic field, rotating about its axis. The rotation is due either to the $J \times B$ Lorentz force, where J is the radial discharge current density and B is the axial magnetic field, or to the $E \times B$ drift, where E is a self-sustained radial electric field in the plasma column.

The main body of work that has been done on isotope separation in the plasma centrifuge consists of studies in partially ionized plasmas. Only low degrees of enrichment were achieved due to the deleterious effect of the neutrals [4]. These effects were avoided in the fully ionized plasma centrifuge developed recently [5]. The fully ionized plasma column was produced in a magnetized pulsed vacuum arc of several kiloamps peak current and ~1 ms RC decay time. In addition to the description of the experimental apparatus, [5] includes a simplified theoretical model which could be applied to a two-ion-component plasma.

In this paper we describe further experimental results of the fully ionized plasma centrifuge, obtained in a larger apparatus, with 6–12 ms constant-current vacuum arc pulses in axial magnetic fields of up to 5 kG. We also present an improved multicomponent theoretical model of the plasma centrifuge and compare it with the experimental results. The remainder of this paper is arranged as follows. The experimental apparatus is described in Section II. In Section III measurement results of various parameters of the plasma centrifuge, including rotation, plasma density, and mass enrichment are presented. The theoretical model is in Section IV, followed by a discussion in Section V. The paper is concluded by a short summary given in Section VI.

II. Experimental System

The experimental system is illustrated in Fig. 1. It consists of a 4-m-long 30-cm-diameter cylindrical metal chamber inside the bore of a set of electromagnet coils. The axial magnetic field region, of up to 5 kG, is uniform to ±1 percent over a length of 2.6 m and ±1 percent over the chamber diameter.

The chamber is pumped by two 1500 l/s turbo-molecular pumps (TMP's), one at each end, to a pressure of 10^{-6}–10^{-7} torr. At one end of the chamber is the cathode assembly, which includes a water-cooled stainless steel stem, inserted through the end flange, with the cathode mounted on it. The stem length is such that the cathode is positioned in the constant magnetic field region. The cathode is connected to an impedance-matched 70-mΩ pulse-forming network (PFN), which produces a relatively flat-topped current pulse of 6–12-ms duration and up to 4 kA. This network can deliver more than 50 percent of its stored energy into the vacuum arc. Approximately 5–10 cm in front of the cathode face is a grounded tungsten mesh, which serves as an anode. A trigger electrode

Manuscript received July 13, 1986; revised February 25, 1987. This work was supported by the Office of the Chief Scientist, Ministry of Industry and Trade, Israel, and by the Israel Isotopes Partnership.

M. Geva, O. Danziger, L. A. Levin, and S. Maharshak are with Isomed Ltd., Jerusalem 91230, Israel.

C. Cohen, F. Dothan, L. Friedland, and J. L. Hirshfield are with Isomed Ltd., Jerusalem 91230, Israel, and with Hebrew University of Jerusalem, Jerusalem, Israel.

IEEE Log Number 8716630.

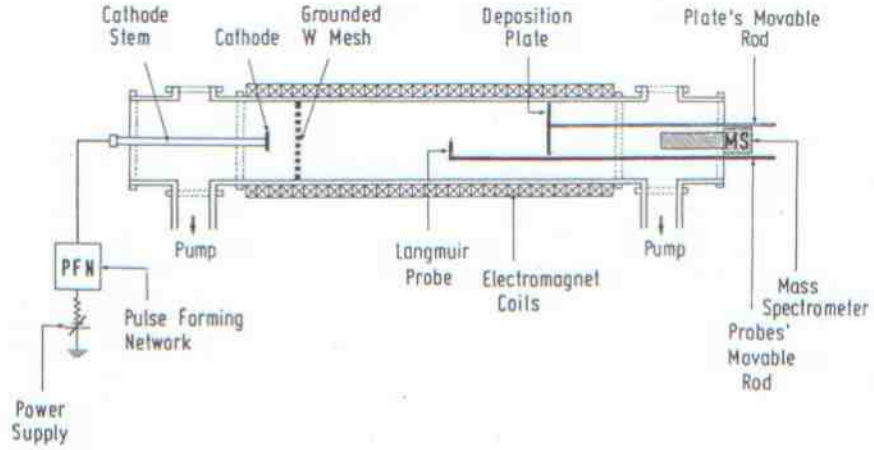

Fig. 1. Schematic of plasma centrifuge.

passes through a 10-mm hole at the center of the cathode and the stem, and is surrounded by a quartz sleeve with its face slightly in front of the cathode face. When a high-voltage pulse is applied between the two electrodes, a breakdown occurs and the small plasma plume emitted there triggers the main vacuum arc.

At the other end of the chamber, a quadrupole mass spectrometer (VG MS 12-12) is connected on axis and serves to analyze with time resolution of 10 u/ms the plasma composition on the discharge axis. In addition to the mass spectrometer, Langmuir probes are inserted into the chamber through the end flange. The probe consists of a metal wire covered by a nonconducting sleeve (such as glass), with only its tip exposed. The probe is positioned in the plasma and is electrically "floating" by connection to a high-impedance amplifier input. A total of four probes were inserted into the chamber in two pairs, each pair in one axial position with the probes 90° to each other. The axial and radial positions of each pair of probes could be changed manually.

A collecting plate could also be introduced into the chamber at axial positions over a 2-m range. The material deposited on this plate was then analyzed to give the radial thickness profile of the deposition, using a polarization interferometer (see further details in [5]), or the chemical composition of the deposition, as a function of radius, using an energy-dispersive X-ray spectrometer (EDX: Tracor-Northern, TN-5500) attached to a scanning electron microscope (SEM: JEOL 35CF), where high-energy electrons of the SEM impinge on a surface, causing characteristic X-ray line emission from a layer of ~ 1-μm depth. This emitted radiation is analyzed according to its energy and intensity, thus providing reliable quantitative information of the surface chemical composition. The EDX is not sensitive, however, to different isotopes of the same chemical element due to its limited resolution. It was necessary, therefore, to use plasmas of more than one chemical component, such as Cu–Ni and Cu–Zn, when studying the radial enrichment profile.

III. Experimental Results

A. Plasma Rotation

To measure the rotation in this study, two main diagnostics were used. The first was the Langmuir probe, described in Section II. Fig. 2(a) shows signals of the arc current (measured as the voltage drop across a 1-mΩ low-inductance shunt) of about 2 kA and 6-ms duration (upper trace) and of two probes (lower traces) which were positioned at $r = 3$ cm and at 90° to one another in the plasma column. The probe signals show a typical curve of floating probe potential in a plasma with superimposed periodic fluctuations due to the plasma rotation (density variations). Fig. 2(b) shows an expanded section of the probe signals, showing clearly the periodic fluctuations and the quarter-period shift of the two signals. Fig. 2(c) shows the Fourier transform of the probe signal (performed by a Nicolet 4094/4562/XF-44 digital oscilloscope system), showing that the spectrum has a pronounced peak at a plasma rotation frequency of 10^5 rad/s. Probe signals from different radii and axial positions indicated a solid-body rotation of the plasma column.

The second diagnosis was done by inserting a plexiglass plate across the plasma, with a 4-mm-wide slit along its diameter and a second plexiglass plate 4 cm behind it. The rotating plasma passed through the slit and continued its rotation until it arrived at the second plate and deposited on it, as shown in Fig. 3, shifted by an angle of about 25° to the slit. The axial velocity of the plasma was measured to be $\sim 10^6$ cm/s [5]. Using this value, the deposition indicated a rotation frequency of $\sim 10^5$ rad/s, in good agreement with the probe measurement of 0.9–$1.2 \cdot 10^5$ rad/s. After reversing the axial magnetic field, the deposition through the slit indicated a reversal of the plasma rotation, as expected.

Measurements of the plasma rotation in Cu, Cu–Ni, Cu–Zn, Co, Cu–Co, and Co–Fe plasmas showed rotations of 0.7–$1.2 \cdot 10^5$ rad/s, in good agreement with the previous results [5].

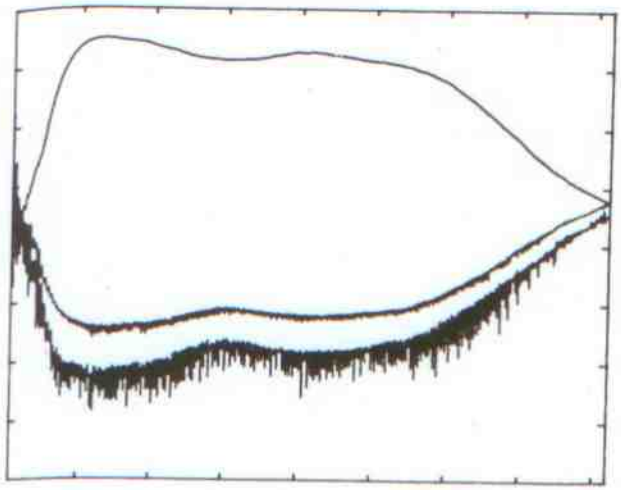

TIME (1.25 msec/div)
(a)

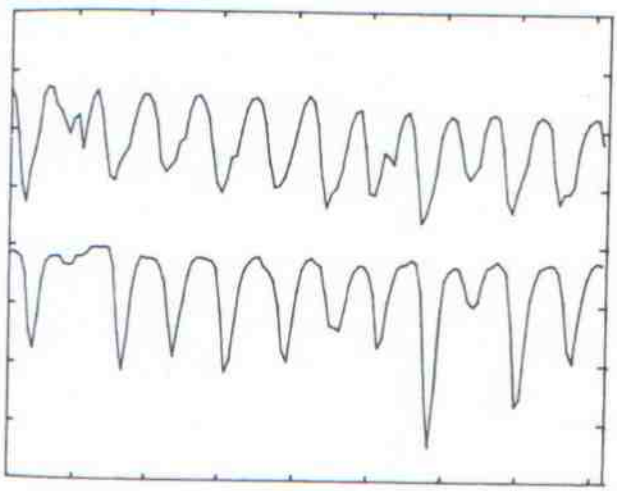

4.6 msec TIME (80 μsec/div)
(b)

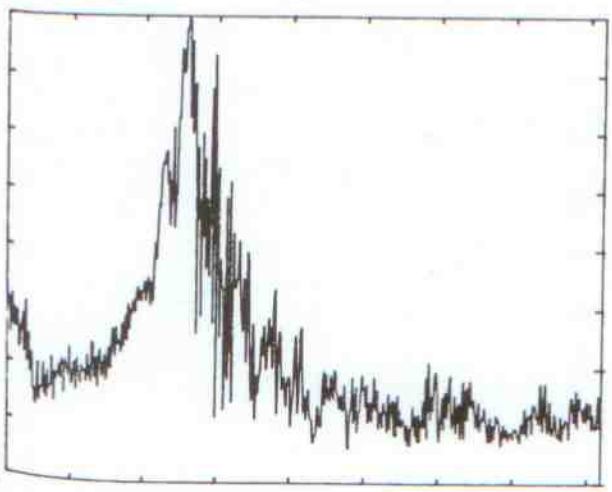

FREQUENCY (6.7 kHz/div)
(c)

Fig. 2. (a) Current (upper trace) and probe (lower traces) signals in Cu arc. The current pulse is ~2 kA for ~6 ms. (b) Expanded section of the probe signals, showing the quarter-period delay. (c) Fourier transform of the probe signal, indicating angular velocity of $\sim 10^5$ rad/s.

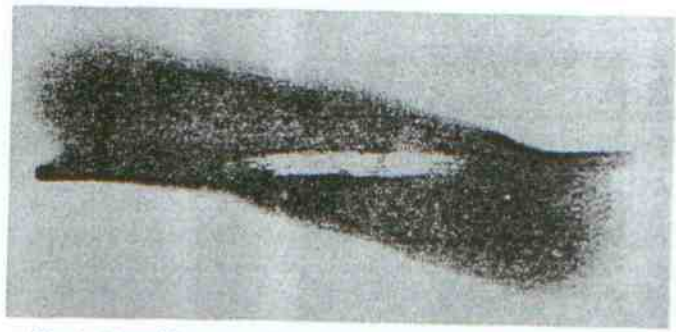

Fig. 3. Deposition trace of the rotating plasma through a 4-mm slit.

B. Plasma Density

To measure the radial plasma density profile, advantage was taken of an experimental finding, that the plasma axial velocity is rather radius independent inside the plasma column. The thickness of the plasma material deposited on a plate across the plasma column is therefore proportional to the plasma density, and by measuring this thickness versus radius, one obtains the radial density profile of the plasma. The thickness of the deposited layer was measured using polarization interferometry, as described in [5]. Fig. 4 shows a radial density profile of a Cu–Zn plasma with $I = 1.5$ kA and $B = 1.3$ kG, measured 2.2 m from the cathode. The total mass deposited in the column and the total mass loss from the cathode per discharge pulse were measured by weighing the cathode and collecting substrate before and after the discharge series. In the present configuration, about 170–190 μg of cathode material was deposited per pulse, which was about one-third of the mass loss from the cathode per pulse. No effort has been made to maximize this fraction.

Deposition of 180 μg/pulse in Cu–Ni plasma, with pulse length of $6 \cdot 10^{-3}$ s, plasma axial velocity of $\sim 10^6$ cm/s, and plasma diameter of 6 cm corresponds to average ion density of 10^{13} cm^{-3} on axis, in agreement with previous measurements [5].

The radial plasma-density profiles, which were obtained as described above under various conditions, revealed that the plasma diameter depends mainly upon the axial magnetic field up to $B = 1.5$–2 kG. Above this value the dependence is very weak. There is also a weak dependence on the axial position and some dependence on the arc current. The column diameter seems independent of the cathode material.

C. Mass Enrichment in the Plasma Centrifuge

The mass spectrometer could be mounted, in the existing system, only on axis to measure the ion composition at the center of the plasma. In this configuration there was no reliable way to probe the plasma composition at radii off axis, since directing ions from large radii to the mass spectrometer entrance-orifice on center, across magnetic field lines, changes their relative abundance. The mass spectrometer was thus used to check the ion composition on axis and particularly to look for depletion of the heav-

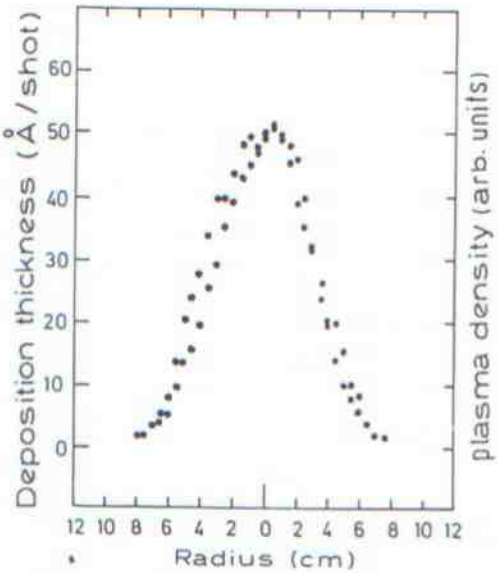

Fig. 4. Radial profile of the deposited-layer thickness (proportional to plasma density) in Cu–Zn arc.

ier ion relative to the lighter one, which should accompany any enrichment at the outer radii.

Fig. 5 shows the mass spectrometer spectra of Cu^+ isotopes. The upper spectrum was taken when the probes indicated a plasma rotation frequency of $\sim 10^5$ rad/s. It shows a ratio of $^{63}Cu^+/^{65}Cu^+ \simeq 4$. The lower spectrum was taken when the plasma did not rotate regularly and the ratio is the natural 2.2.

To find the enrichment versus radius, the EDX was used to analyze, at various radii, the material deposited by a two-element plasma on a collecting plate which was positioned across the column inside the constant magnetic field region.

Fig. 6 shows the enrichment factor q versus radius for Cu–Ni plasma, as measured by the EDX, where q is defined as the ratio of the Cu and Ni densities at radius r minus their ratio on axis ($r = 0$), divided by the ratio on axis:

$$q(r) = \frac{n_{Cu}(r)/n_{Ni}(r)}{n_{Cu}(0)/n_{Ni}(0)} - 1.$$

The Cu–Ni cathode was made of constantan alloy (Cu : Ni–70 percent : 30 percent). The arc current was 1.5 kA and the axial magnetic field was 4 kG.

Mass enrichment was also studied in plasmas of Cu–Co and Cu–Zn. Zn enrichment of up to 300 percent was measured in a Cu–Zn plasma with an axial magnetic field of 1.3 kG.

D. Radial Profile of the Floating Potential

The potential of a floating Langmuir probe in an isothermal plasma with constant magnetic field differs by an additive constant from the plasma space potential [6]. Thus, the radial profile of the floating potential is identical in shape to the radial profile of the plasma space potential and shifted in its magnitude. Therefore, the radial

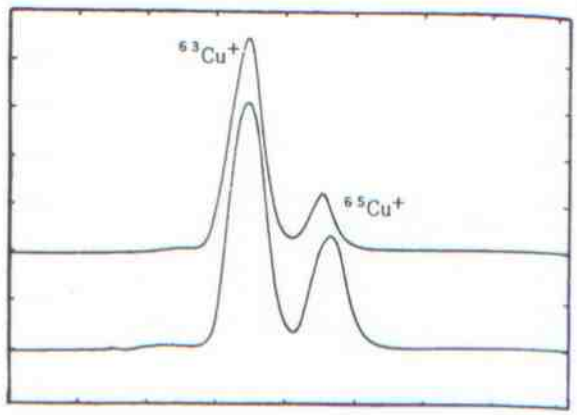

Fig. 5. Mass spectrometer spectrum of Cu^+ isotopes. The upper spectrum was taken when the plasma rotated with $\omega = 10^5$ rad/s. The lower spectrum was taken with a nonrotating plasma.

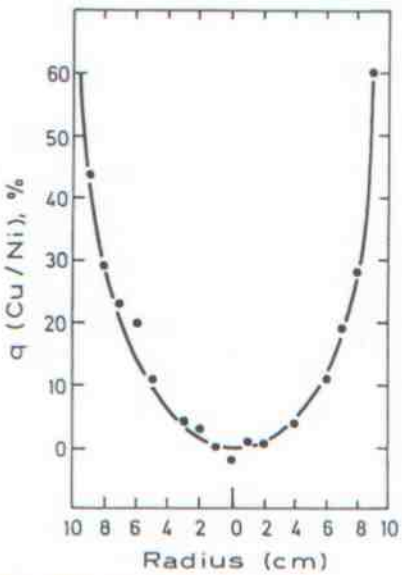

Fig. 6. Radial profile of the enrichment factor in Cu–Ni plasma.

electric field in the plasma column can be inferred from it. The floating probe potential on axis was negative and increased quadratically with radius, becoming positive at the column edge, and then decreased to zero towards the chamber wall. Fig. 7 shows a radial profile of a plasma potential, as well as the radial density profile of a Cu–Ni plasma with $B = 1.3$ kG. Within the plasma column the potential depends quadratically on the radius, whereas it changes only slightly axially. Hence, the electric field within the column is radial, pointing inward, and its magnitude increases linearly with the radius, as expected in a plasma column rotating with solid-body rotation. The value of the rotational $\boldsymbol{E} \times \boldsymbol{B}$ drift velocity is compared in Fig. 7 with the measured value. The good agreement shows that the $\boldsymbol{E} \times \boldsymbol{B}$ drift produces the rotation of the plasma column.

IV. Theoretical Model

The model presented below describes the steady-state equilibrium of a rotating magnetized plasma column con-

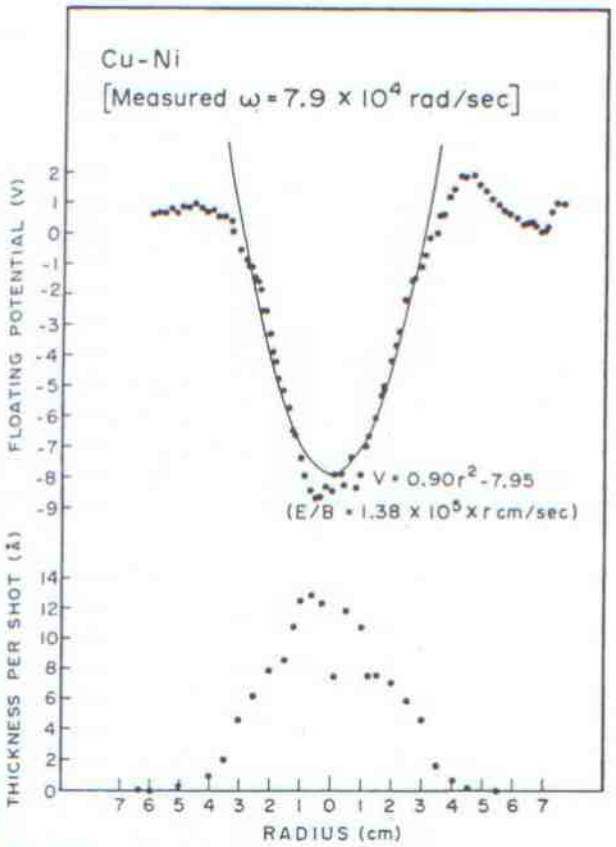

Fig. 7. Radial profile of the probe floating potential (upper trace) and of the plasma density (lower trace) in a Cu–Ni plasma.

sisting of several ion species in different ionization states. The basic fluid approximations of [5] are adopted here, but are generalized to an arbitrary number of ion species and arbitrary axisymmetric electron radial density profiles. We assume a fully ionized plasma where the ions rotate together as a solid body with rotation frequency ω. The ion temperature is assumed to be independent of time and space coordinates. Ion–electron collisions are neglected, i.e., we assume the electrons to be bound to the magnetic field lines with no radial diffusion, and the radial electron density profile does not change axially. The collisions between different ion species lead to a centrifugal redistribution of the isotopic masses and ionization states within the plasma column. The ion density distribution is determined radially by a balance between centrifugal, pressure gradient, electrostatic, and Lorentz forces and is independent of the time and axial coordinates. Thus, the radial distribution of ion species, labeled i, is given by a Boltzmann law

$$n_i(r) = n_i(0) \exp\left\{\left[-Z_i e\phi(r) + \tfrac{1}{2} M_i \omega^2 r^2 + \tfrac{1}{2} Z_i e\omega B r^2\right]/kT\right\} \quad (1)$$

while the electrons obey a similar law

$$n_e(r) = n_e(0) \exp\left\{\left[e\phi(r) - \tfrac{1}{2} e\omega_e B r^2\right]/kT_e\right\} \quad (2)$$

where the centrifugal contribution is negligible since $m/M_i \ll 1$, and where $\omega_e \neq \omega$ is the electron's azimuthal rotation frequency.

If $n_e(r)$ is a specified function (set by boundary conditions outside of the regime of competence of this equilibrium theory), e.g.,

$$n_e(r) = n_e(0) \exp\left[-f(r)\right] \quad (3)$$

with $f(0) = 0$ and $f(r) > 0$ for $r > 0$, then $\phi(r)$ and $\omega_e(r)$ are related through

$$f(r) = \left[-e\phi(r) + \tfrac{1}{2} e\omega_e(r) B r^2\right]/kT_e. \quad (4)$$

But for typical experimental conditions,

$$f(r) \ll \tfrac{1}{2} e\omega_e(r) B r^2/kT_e \simeq 10r^2 \ (r \text{ in cm}). \quad (5)$$

Thus, one finds that approximately

$$\phi(r) \simeq \tfrac{1}{2} \omega_e(r) B r^2 \quad (6)$$

$$\omega_e(r) \simeq E(r)/rB \quad (7)$$

so that it is the electrons which exhibit a nearly pure $E \times B$ drift, while the ions, in response to the overall balance of forces, rotate at a lower frequency ω.

One must observe local charge balance

$$n_e(r) = \sum_i Z_i n_i(r) \quad (8)$$

as well as the normalization requirement

$$Z_i \int_0^\infty dr\, r n_i(r) = u_i \int_0^\infty dr\, r n_e(r) \quad (9)$$

wherer u_i is the overall abundance in the plasma for isotopic species i of given charge state Z_i. Equation (8) for a given $n_e(r)$ can be viewed as an implicit functional relationship

$$F[\phi(r), r] = 0 \quad (10)$$

which can be numerically solved for $\phi(r)$, thus for the individual ion distributions (see (2)). One can find $\phi(r)$ by using the continuation method. Implicit differentiation of (10) gives

$$d\phi(r)/dr = -(\partial F/\partial r)/(\partial F/\partial \phi). \quad (11)$$

Equation (11) can be solved numerically, by starting with $\phi(0) = 0$ and by guessing an initial abundance of the ions at $r = 0$. The ion abundance at the axis can then be iterated until the integral condition (9) is satisfied to the desired accuracy. The quantities U_i, M_i, Z_i, ω, B, T, and $n_e(r)$ should be specified based on their measured values. For a two-component plasma of a single ionization state, these equations lead to the familiar result (see [5])

$$q_0 = \exp\left[\omega^2 r^2 \Delta M/2kT\right] \quad (12)$$

where ΔM is the mass difference of the two ion species.

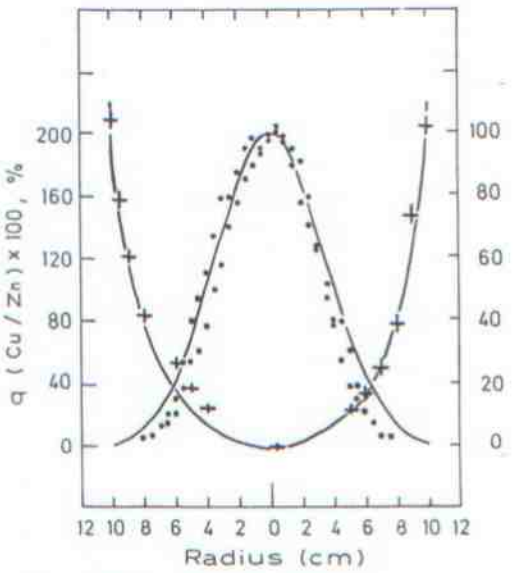

Fig. 8. Radial enrichment factor and radial plasma density profile in Cu–Zn plasma.

V. Discussion

Although the measured radial density profile of the plasma does not exactly match a Gaussian shape, this seems to be a good approximation for the radial electron density profile and was used in most of our theoretical calculations. The full width at half maximum (FWHM) of the Gaussian was taken as that of the measured density distribution profile. The on-axis mass spectrometer was used to measure the ionization states in the plasma column. Under the conditions of our system, the plasma was found to be singly ionized. For the various parameters in the model we used the measured values, except for the ion temperature, which we had not measured. We assumed a value of $T = 1$ eV, as measured by others (see [5]).

A comparison between the experimental results and theoretical prediction is shown in Fig. 8 for the radial enrichment factor q of Zn and the radial plasma density profile in a plasma of Cu (60 percent) and Zn (40 percent). The plasma parameters were $\omega = 10^5$ rad/s (measured), FWHM = 8.3 cm (measured), $B = 1.3$ kG, and $T = 1$ eV. The curves represent the theoretical model prediction. The Zn density at each radius is the sum of the individual densities of its isotopes there, and so is the Cu density. The measured enrichment was found using the EDX analysis. There is a good agreement between the experimental results and the theoretical curves. The model indicates that although the radial electron, and therefore the plasma density, distribution is Gaussian, the individual distributions of the various isotopes are not necessarily Gaussian. Clearly, the EDX measurement of enrichment in a two-element plasma centrifuge, presented in this paper, should be complemented by an analysis of a single-element isotope enrichment.

The linear dependence on radius of the radial electric field within the plasma column agrees well with a solid body rotation of the plasma, caused mainly by the $E \times B$ drift. This, together with the exponential dependence of the mass-enrichment factor on the square of the rotational velocity, indicates the importance of increasing the radial electric field across the plasma column in order to increase the separation factor in the centrifuge. The property of the plasma of effectively shielding externally imposed electrostatic fields limits the ways of influencing the self-sustained radial electric field. Various parameters, such as the geometry and boundary conditions at the cathode–anode region, may play an important role.

The radial electric field in the column is due to slight charge separation within the column, which may be caused by the electrons being bound to the magnetic field lines more tightly than the ions, with their larger Larmor radii.

VI. Conclusion

A reliable generation of fully ionized regularly rotating plasma columns of Cu, Cu–Ni, Cu–Zn, and others has been demonstrated. The plasma was produced by a 6–12-ms 1–4-kA constant current pulsed vacuum arc in a constant magnetic field of up to 5 kG. The radial plasma density roughly followed a Gaussian profile, with 10^{13}-cm^{-3} peak density. The radial electric field in the column was shown to point inward and grow linearly with the radius, indicating the rotation to be mainly due to the $E \times B$ drift. Centrifugal mass enrichment of up to 300 percent was produced in a Cu–Zn plasma. An improved multispecies multi-ionization state theoretical model was developed, which calculates the individual radial density profiles for the various ion species in a steady-state equilibrium plasma centrifuge.

Acknowledgment

The authors would like to thank M. Matatyahu for his skillful engineering support in all of these experiments.

References

[1] J. Slepian, "Failure of the ionic centrifuge prior to the ionic expander," *J. Appl. Phys.*, vol. 26, p. 1283, 1955.

[2] B. Bonnevier, "Experimental evidence of element and isotope separation in a rotating plasma," *Plasma Phys.*, vol. 13, pp. 763–774, 1971.

[3] B. Lehnert, "Rotating plasma," *Nucl. Fusion*, vol. 11, pp. 485–533, 1971.

[4] M. M. B. Wijnakker and E. H. A. Granneman, "Limitations on mass separation by the weakly ionized plasma centrifuge," *Z. Naturforsch.*, vol. 35A, pp. 883–893, 1980.

[5] M. Geva, M. Krishnan, and J. L. Hirshfield, "Element and isotope separation in a vacuum-arc centrifuge," *J. Appl. Phys.*, vol. 56, pp. 1398–1413, 1984.

[6] R. H. Huddleston and S. L. Leonard, Eds., *Plasma Diagnostic Techniques*. New York: Academic, 1965, ch. 4.